Criticality of Two-Dimensional Disordered Dirac Fermions in the Unitary Class and Universality of the Integer Quantum Hall Transition

Björn Sbierski, Elizabeth J. Dresselhaus, Joel E. Moore, and Ilya A. Gruzberg

Phys. Rev. Lett. **126**, 076801 — Published 18 February 2021

DOI: 10.1103/PhysRevLett.126.076801

Criticality of two-dimensional disordered Dirac fermions in the unitary class and universality of the integer quantum Hall transition

Björn Sbierski,[1] Elizabeth J. Dresselhaus,[1] Joel E. Moore,[1,2] and Ilya A. Gruzberg[3]

[1] *Department of Physics, University of California, Berkeley, California 94720, USA*
[2] *Materials Sciences Division, Lawrence Berkeley National Laboratory, Berkeley, California 94720, USA*
[3] *Ohio State University, Department of Physics, 191 West Woodruff Ave, Columbus OH, 43210*

(Dated: January 25, 2021)

Two-dimensional (2D) Dirac fermions are a central paradigm of modern condensed matter physics, describing low-energy excitations in graphene, in certain classes of superconductors, and on surfaces of 3D topological insulators. At zero energy $E = 0$, Dirac fermions with mass m are band insulators, with the Chern number jumping by unity at $m = 0$. This observation lead Ludwig *et al.* [Phys. Rev. B **50**, 7526 (1994)] to conjecture that the transition in 2D disordered Dirac fermions (DDF) and the integer quantum Hall transition (IQHT) are controlled by the same fixed point and possess the same universal critical properties. Given the far-reaching implications for the emerging field of the quantum anomalous Hall effect, modern condensed matter physics and our general understanding of disordered critical points, it is surprising that this conjecture has never been tested numerically. Here, we report the results of extensive numerics on the phase diagram and criticality of 2D-DDF in the unitary class. We find a critical line at $m = 0$, with energy-dependent localization length exponent. At large energies, our results for the DDF are consistent with state-of-the-art numerical results $\nu_{\mathrm{IQH}} = 2.56$–$2.62$ from models of the IQHT. At $E = 0$ however, we obtain $\nu_0 = 2.30$–2.36 *incompatible* with ν_{IQH}. This result challenges conjectured relations between different models of the IQHT, and several interpretations are discussed.

Introduction. The integer quantum Hall effect appears when a two-dimensional (2D) electron gas is placed in a strong perpendicular magnetic field. Without disorder, the electron eigenstates form Landau levels, and each filled level contributes unity to the total Chern number C. Disorder is essential for experimental observation of the (dimensionless) quantized Hall conductivity $\sigma_{xy} = C$; it broadens the Landau levels into bands and localizes eigenstates on a scale $\xi(E)$ that diverges as a power law at a critical energy E_c [1], $\xi(E) \sim |E - E_c|^{-\nu_{\mathrm{IQH}}}$. For Fermi energies $E \neq E_c$ and system sizes $L \gg \xi(E)$ the Hall conductivity is quantized. The integer quantum Hall transition (IQHT) at $E = E_c$ is the most studied Anderson transition [2] because of its conceptual simplicity, low dimensionality, and experimental relevance. However, critical properties at the IQHT are notoriously difficult to compute analytically; they are mostly known from numerical studies which employed the Chalker-Coddington (CC) network model [3–13], microscopic continuous [14, 15], lattice [10, 14–17], and Floquet Hamiltonians [18]. In recent works, the critical properties agree between models, indicating universality of the IQHT. They include the localization length exponent $\nu_{\mathrm{IQH}} = 2.56$–$2.62$ and the leading irrelevant exponent $y \simeq 0.4$ (with large error bars). At criticality, y describes the approach of the dimensionless quasi-1D Lyapunov exponent Γ to its limiting value at infinite system size $\Gamma_0^{\mathrm{IQH}} = 0.77$–$0.82$ [5–7, 9, 11–13, 16]. A similar exponent y was found for the average conductance $\overline{g}$ of a square sample with limiting value $\overline{g}_{\mathrm{IQH}} = 0.58$–$0.62$ [19, 20]. For ongoing analytical work on the IQHT, see [21–23] and the discussion below. The IQHT has also been discussed recently in relation to exotic topological superconductor surface states [24].

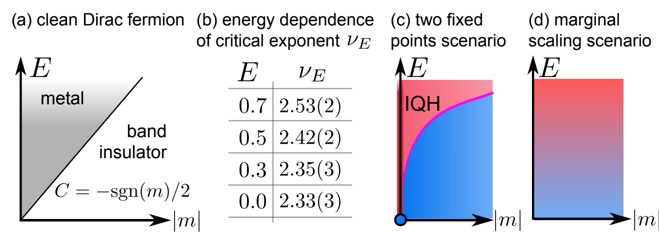

FIG. 1. Schematic phase diagram for 2D Dirac fermions. (a) Clean case: A metal intervenes between two band insulators with different Chern numbers C at $|m| > |E|$. With disorder in the unitary class, the metal localizes except on the critical line $m = 0$ separating topologically distinct Anderson insulators. (b) The critical exponent ν_E is found to vary significantly with energy. The two fixed points scenario (c) explains this as a result of a crossover, while the marginal scaling scenario (d) would be compatible with a smooth evolution of effective critical exponents.

A longstanding conjecture by Ludwig *et al.* [25] states that the IQHT fixed point also controls the criticality of 2D disordered Dirac fermions (DDF). The clean Dirac Hamiltonian is

$$H_0 = \hbar v \left(-i\sigma_x \partial_x - i\sigma_y \partial_y\right) + m\sigma_z, \qquad (1)$$

with Pauli matrices σ_μ, mass m, and velocity v. The spectrum of H_0 has a gap $2|m|$ symmetric around $E = 0$. For Fermi energies E within the gap, the system is a band insulator with half-integer quantized $\sigma_{xy} = C(m) = -\frac{1}{2}\mathrm{sgn}(m)$ [25], see Fig. 1(a). If the Dirac fermion is regularized on a lattice as in the Haldane model [26] or

Eq. (5) below, H_0 only describes the low-energy excitations near a certain point in the Brillouin zone. Bloch states elsewhere contribute another 1/2 to C, such that $|\sigma_{xy}|$ jumps between zero and one as m changes sign.

With m taking the role of energy, the superficial similarity of this transition to the IQHT motivated Ludwig *et al.* [25] to consider the effects of disorder in the unitary symmetry class [27, 28],

$$H = H_0 + \sum_{\mu=0,x,y,z} U_\mu(x,y)\sigma_\mu. \qquad (2)$$

The random scalar (U_0) and vector ($U_{x,y}$) potentials, and the random part of the mass (U_z) are taken to be independent Gaussian fields with the correlators $\overline{U_\mu(\mathbf{r})U_\nu(\mathbf{r}')} = \delta_{\mu\nu}K_\mu(|\mathbf{r}'-\mathbf{r}|)$ and zero mean. Time reversal changes the sign of $m+U_z$, connecting two equally likely members of the statistical ensembles with opposite values of m, and the transition in the disordered model happens at $m=0$. Due to the absence of an extended 2D metal phase in the unitary class, all eigenstates of H with $|m|>0$ are expected to be localized with the localization length $\xi(m) \sim |m|^{-\nu_E}$, with a possibly E-dependent critical exponent ν_E.

Although model (2) is not solvable analytically, the conjecture [25] $\nu_{\mathrm{E}=0} = \nu_{\mathrm{IQH}}$ was based on a semiclassical argument that leads to the CC-model. Another argument [29] considers the clean CC-model and finds a Dirac spectrum, but the inclusion of disorder is uncontrolled. In the supplemental material (SM) [30], we review these arguments and identify their possible flaws.

Despite the importance of the 2D Dirac model in modern physics, the conjectured emergence of IQHT criticality in DDF was never checked numerically. Here, we address this issue with extensive simulations employing different microscopic models and scaling observables. We start with the continuum model (2) and use the transfer matrix (TM) approach in quasi-1D (q1D) geometry to find the critical behavior near the line $m=0$ in the m-E plane, see Fig. 1(b). At large E our results are consistent with $\nu_E = \nu_{\mathrm{IQH}}$, but as E is lowered, the critical exponent decreases towards $\nu_{E=0} = 2.33(3)$ still close to, but strikingly *incompatible* with ν_{IQH}. We corroborate our $E=0$ results in a lattice model of DDF, employing an alternative 2D scaling observable [10].

In the experimental literature, a quantized non-zero σ_{xy} in the absence of an external magnetic field is known as the quantum anomalous Hall effect [31–33]. Recent efforts [34, 35] have been directed to the critical scaling at the topological phase transition in question, however, the error bars on the resulting exponents are still large.

Continuum model and disorder-induced length scale. We start with Hamiltonian (2) at $E=0$ and smooth disorder, $K_\mu(r) = W^2 e^{-r^2/2a^2}/2\pi$. We use the disorder correlation length a and $\hbar v/a$ as units of length and energy so that the dimensionless disorder strength W, taken to be the same for all four disorder fields, is the bare energy scale in the model. The mean free path l_W equals the quasiparticle decay time, $l_W \equiv -1/\mathrm{Im}\,\Sigma_{\uparrow\uparrow}(0,0)$ defined in terms of the disorder-averaged Green function $\overline{G(\mathbf{k},\omega)} = [\omega - H_0(\mathbf{k}) - \Sigma(\mathbf{k},\omega)]^{-1}$. For weak disorder $W \ll 1$, a perturbative renormalization group (RG) [25, 36] gives, for $m=0$, $l_W \propto e^{c/W^2}$, with $c = O(1)$. To ensure that our system sizes $L \gg l_W$, we work with strong disorder $W \geq 1.5$ where a numerically exact method [37] yields $l_{W=1.5} = 1.54$. We also observe that for $kl_W > 1$, the peaks in the spectral function $A(\mathbf{k},\omega) = -\frac{1}{\pi}\mathrm{tr}\,\mathrm{Im}\,\overline{G(\mathbf{k},\omega)}$ occur at frequencies $\omega \simeq \pm\hbar v k$, i.e. the velocity v is almost un-renormalized. We conclude that for $W=1.5$, system sizes $L \gtrsim O(10)$ are large enough to exhibit disorder-dominated physics.

Lyapunov exponent (LE). A common method to analyze critical behavior in disordered systems employs the self-averaging LEs γ_i in a quasi-1D geometry with length $L_x \to \infty$ [38]. The smallest $\gamma_i > 0$ (the inverse of the 1D localization length) gives the scaling variable $\Gamma = \gamma L_y$, which increases (decreases) with width L_y in a localized (extended) phase and is scale-invariant at a critical point. Following Ref. [39], we use finite $L_x = O(10^5)$ and find Γ as the average over hundreds of disorder realizations, see SM for details.

The eigenvalue problem for the DDF (2) can be rewritten as $\partial_x\psi(x,k_y) = f(\psi(x,k_y'))$. The right hand side contains scattering between transversal wavevectors k_y but is local in x, which allows us to express the TM in exponential form. We impose periodic boundary conditions (BC) in the y direction. We discretize the x direction and stabilize the TM multiplication by repeated QR-decompositions [1] (to obtain Γ) or via a scattering matrix [40] (for the conductance of moderately sized systems). Both methods are numerically exact and faithfully treat model (2) without band bending or node doubling. The only approximations are related to the cutoff $|k_y| \leq k_{\max}$ and the x-discretization. The associated length scales (taken equal) were chosen much smaller than a, and results are converged with respect to these parameters.

Results for the dimensionless LE Γ at $E=0$, $W=1.5$, various masses m and system widths L_y are presented in Fig. 2. The solid lines are fits to the scaling function

$$\Gamma(m, L_y) = \Gamma_0 + \alpha_{01}L_y^{-y} + \alpha_{20}m^2 L_y^{2/\nu}, \qquad (3)$$

which is the lowest-order polynomial ansatz allowed by symmetry, including an irrelevant contribution. The fit gives the following critical properties:

$$\nu_{E=0} = 2.32(1), \quad y = 0.51(3), \quad \Gamma_0 = 0.84(1), \qquad (4)$$

the number in parentheses denotes one standard deviation. In the SM, we give a detailed account for the fitting procedure and show its stability with respect to higher order terms in Eq. (3) and a removal of data points

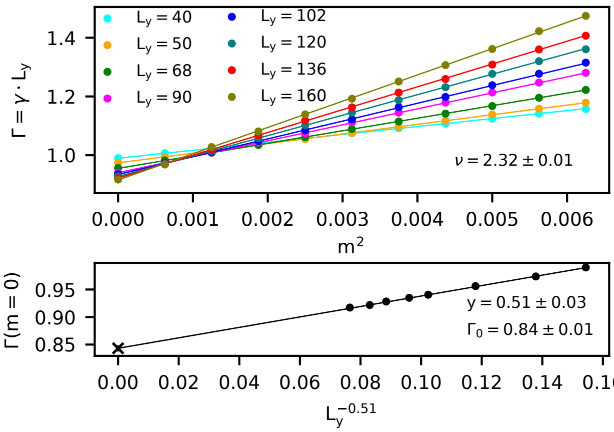

FIG. 2. Top: LEs Γ for $E = 0$ and $W = 1.5$ as functions of m^2. The relative error is $\leq 0.2\%$, error bars are smaller than the dots. Solid lines denote the best fit [Eq. (3)] with fit parameters as given in the panels. Bottom: Closeup at criticality ($m = 0$) with extrapolation to infinite system size determining Γ_0 (cross).

for large m and small L_y. There, we also present data for an increased disorder strength $W = 2.0$, which yields $\nu_{E=0} = 2.31(2)$, $y = 0.51(3)$ and $\Gamma_0 = 0.84(1)$ compatible with anticipated disorder-independent critical properties.

Lattice model and alternative scaling observable. We now confirm the value of $\nu_{E=0}$ using a square-lattice regularization of the DDF allowing access to an alternative scaling observable introduced by Fulga *et al.* [10]. In momentum space, the clean model reads [41]

$$H_0^L = \sigma_x \sin k_x + \sigma_y \sin k_y + \sigma_z(m - 2 + \cos k_x + \cos k_y), \quad (5)$$

where lattice constant and energy scale have been set to unity. For $|\mathbf{k}| \ll 1$, this model reduces to Eq. (1), with a topological transition at critical $m = m_c = 0$ where C changes by 1, but band bending is important for $k, E \gtrsim 1$. We add on-site disorder potentials, $V = \sum_{\mathbf{r}_i,\mu} U_\mu(\mathbf{r}_i)\sigma_\mu$ with $U_\mu(\mathbf{r}_i)$ uniformly drawn from the interval $[-w/2, w/2]$ independently for each lattice site $\mathbf{r}_i$ and $\mu = 0, x, y, z$. Transport calculations use the KWANT package [42] and employ two identical leads attached at the left and right boundaries of the system, represented by decoupled 1D chains extending in the x-direction:

$$H_{Lead}(k_x, k_y) = \sigma_x \sin k_x + \sigma_z (1 + \cos k_x). \quad (6)$$

The lattice model (5) has no symmetry that ensures $m_c = 0$ in the presence of disorder. However, the Dirac node energy is not renormalized away from $E = 0$. The reason is that the eigenenergies come in pairs $\pm E$. This symmetry carries over to the disorder averaged density of states as long as the average potential disorder $\overline{U_0} = 0$.

To determine the exponent $\nu_{E=0}$, we consider the reflection matrix $r(\phi)$ of the left lead as a function of the phase ϕ of twisted BC in the y direction. For a given

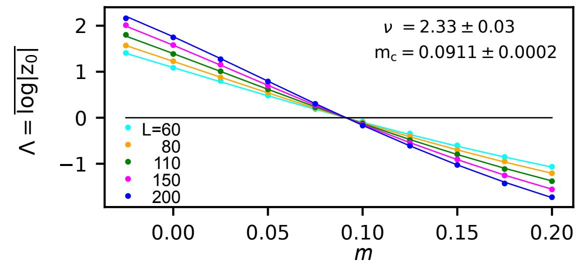

FIG. 3. Scaling plot of the variable Λ for the model (5) at $E = 0$ and disorder strength $w = 2.5$. Dots represent averages over at least 10^4 disorder realizations, and the solid curves are fits described in the SM.

disorder realization, the m_c occurs when there exists a ϕ such that $r(\phi)$ has a zero eigenvalue and $\det r(\phi) = 0$. Fulga *et al.* [10] showed that a scaling observable Λ can be obtained by working with generalized twisted BC $\psi_{x,y=L-1} = z\,\psi_{x,y=0}$ for all $x = 0, 1, ..., L-1$, and $z \in \mathbb{C}$. Now, $\det r(z)$ has zeros z_0 even for $m \neq m_c$ but with $|z_0| \neq 1$. For the z_0 closest to the unit circle, $\Lambda = \overline{\log|z_0|}$ measures the distance to criticality $\Lambda = 0$. For the CC-model, scaling of Λ with system size L was demonstrated in Ref. [10], reporting $\nu = 2.56(3)$ compatible with results from the TM method.

We computed Λ for the lattice DDF $H_0^L + V$ for m around 0, $w = 2.5$ and system sizes between $L = 60$ and 200, see Fig. 3 for the results and the SM for details of the fit. We find $\nu_{E=0} = 2.33(3)$ in agreement with the result for the continuum model. Notably, the observable Λ shows no discernible corrections to scaling, which allows us to omit the irrelevant terms in the scaling function for Λ. Repeating the analysis for $w = 2.25$ and 2.75 (not shown) yields compatible ν within the given error bars.

Results for finite energy ($E > 0$). We now consider the continuum model (2) with smooth disorder at finite energy $E > 0$ ($E < 0$ is related by the statistical $E \to -E$ symmetry). In the SM, we present scaling results for the LE Γ for $E = 0.3, 0.5, 0.7$ at disorder strength $W = 2$. As in the $E = 0$ case we find localizing behavior for any $m \neq 0$. The exponents ν_E, see Fig. 1(b), increase monotonically with E towards $\nu_{E=0.7} = 2.53(2)$, significantly different from $\nu_{E=0}$. Other critical properties (Γ_0 and y) do not seem to vary significantly with E.

To further probe the critical line $m = 0$, we compute the critical Landauer conductance g of $L \times L$ systems with periodic BC in the y direction, and metallic leads modeled as highly doped Dirac nodes [43]. The distribution of g and its moments are expected to be scale-invariant and universal [2, 4], for $E = 0$ it is shown in the SM. In Fig. 4 we present the average conductance $\overline{g}$. We observe that for $E \lesssim 0.3$, $\overline{g} \simeq 0.5$ is almost independent of the disorder strength and E, which we interpret as evidence of proximity to an underlying fixed point. With increasing L, $\overline{g}$ slightly increases, consistent with decreasing $\Gamma(m = 0)$

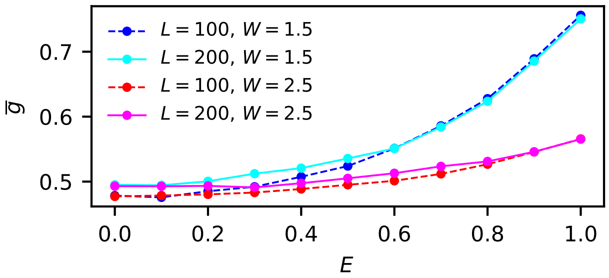

FIG. 4. Critical Landauer conductance $\overline{g}$ of square samples at $m = 0$, disorder strengths $W = 1.5$ and 2.5, size $L = 100, 200$ and periodic BC in transversal direction averaged over at least 10^4 disorder realizations.

in Fig. 2 (bottom).

For $0.3 \lesssim E \lesssim 1$, $\overline{g}$ begins to depend on W, and varies with E by $\sim 50\%$ for $W = 1.5$ but only by $\sim 10\%$ for $W = 2.5$. For $W = 1.5$ and $E > 0.6$, $\overline{g}$ slightly decreases when L grows form 100 to 200. We interpret this as a remnant of the crossover from the diffusive to the critical behavior. It is consistent that LEs obtained in this regime (not shown) cease to obey critical scaling.

Discussion. In summary, our numerical results for DDF are consistent with localized behavior anywhere in the m-E plane except on a critical line $m = 0$, see Fig. 1. At $m = 0$, both the dimensionless LE extrapolated to infinite system size $\Gamma_0 = 0.82$–0.85 and the irrelevant exponent y do not vary significantly with energy or disorder strength below $E \simeq 1$, while the average conductance $\overline{g}$ of fixed-size square samples at stronger disorder varies at most by $\sim 10\%$. In contrast, the localization length exponent ν_E significantly depends on energy, see Fig. 1(b). While $\nu_{E=0.7} = 2.53(2)$ is more or less consistent with the established value for the IQHT $\nu_{\rm IQH} = 2.56$–2.62, the value ν_E significantly decreases with energy down to

$$\nu_{E=0} = 2.30\text{–}2.36, \tag{7}$$

where we took a union over error bars for the two models and two scaling methods we used for $E = 0$.

Let us now put our findings in the context of existing arguments and first discuss the case of large E and low W characterized by a large Drude conductivity $\sigma_{xx}^{\rm D} \gg 1$. In the SM, we numerically confirm that this regime is achievable in the DDF, albeit not for the parameters used for the scaling analysis above. Large $\sigma_{xx}^{\rm D}$ controls the derivation of an effective field theory for the DDF with short-range disorder [44] as it justifies the required saddle point approximation. The resulting non-linear sigma model with θ-term can also be derived for other models of the IQHT: the Schrödinger equation with short-range disorder and strong magnetic field [45, 46], and the CC-model [47, 48]. These relations rationalize our finding of IQHT-like criticality in the DDF at $E = 0.7$. Note, however, that the CC-model lacks the large parameter analogous to $\sigma_{xx}^{\rm D}$, and the derivation of the sigma model for it is uncontrolled, as well as for the DDF at $E \simeq 0$, where $\sigma_{xx} < 1$.

We now discuss three possible scenarios addressing the E dependence of ν_E [see Fig. 1(b)].

(a) Insufficient system size. In the history of IQHT-numerics, refined fitting functions and the ability to study larger systems shifted the value of ν considerably over time. We also cannot exclude that our results for $\nu_{E<0.7}$ are not the true asymptotic values, and further increase in L_y would bring them closer to $\nu_{\rm IQH}$. However, our system sizes, quality of numerical data, and its analysis are comparable to recent work on the IQHT. Also, we do not see a tendency for a drift in ν_E if the minimal L_y involved in the fit is increased from 40 to 68, see SM. Finally, we corroborated our $E = 0$ result (7) at two disorder strengths and with an alternative scaling observable for the DDF on a lattice. Our finding for $\nu_{E=0}$ is also supported by numerical results from a massless DDF in a magnetic field [49]. At strong enough potential disorder, only the critical state deriving from the Landau level at $E = 0$ persists, separating localized states at $E \lessgtr 0$. The scaling of $d\sigma_{xy}/dE|_{E=0}$ and the width of the conductance peak around $E = 0$ with system size gave $\nu \approx 2.3$, but no error bars were provided.

(b) Two fixed points. In a more intriguing scenario our results could be consistent with the existence of two *different* fixed points. One of them is the conventional IQHT fixed point that controls the critical behavior at $E > 0$, while the other fixed point controls the system at $m = 0, E = 0$, see the dot in Fig. 1(c). We conjecture that this fixed point is multicritical, where both m and E are relevant, with the RG eigenvalues $y_m = 1/\nu_{E=0}$ and y_E. The RG flow near this point would resemble that near the tricritical point in the Ising model with vacancies [50]. In this scenario the critical behavior at any $E > 0$ should be the same, and coincide with that for the IQHT. Our observation of intermediate values $\nu_{E=0.3,0.5}$ may stem from the small (or even zero, if E is marginally relevant) value of the crossover exponent y_E/y_m at the multicritical point, resulting in the cusp-like shape of the crossover line in Fig. 1(c) which might cause smearing of ν_E when extracted over a too large range of m. However, concerns about this scenario arise from the absence of any kinks in the Γ vs m^2 data for $E > 0$ (see SM) as well as the apparent energy independence of Γ_0.

(c) Marginal scaling. In a recent development, Zirnbauer [23] proposed a solvable conformal field theory for the IQHT, featuring a fixed point with only marginal perturbations, implying $\nu = \infty$, $y = 0$. In this case, higher order terms in the β-functions for relevant and irrelevant scaling fields (the deviations $\delta\sigma_{xx}$ and $\delta\sigma_{xy}$ of the conductivities from their fixed-point values) could lead to an *effective* critical exponent $\nu_{\rm eff}$ [51] dependent on the bare value of $\delta\sigma_{xx}$. For a slow RG flow of $\delta\sigma_{xx}$, $\nu_{\rm eff}$ could appear scale-independent but vary with the parameters of

the model such as energy, see Fig. 1(d). Ref. [52] reports further study of this scenario in the numerically more convenient framework of the CC-model.

Outlook. We hope our findings will prompt a careful re-examination of criticality at the IQHT and other Anderson transitions. Future work on the critical DDF should address multifractal properties of wavefunctions and compare them to established results for the IQHT [2]. Moreover, working with $N = 3, 5, 7...$ flavors of DDF, the assumption $\sigma_{xx}^{\mathrm{D}} \gg 1$ could be justified even for $E = 0$ and it would be interesting to compute $\nu_{E=0}$ in this case. Further, extension of our methods to DDF in the symmetry classes of the spin and thermal quantum Hall effects is worthwhile.

Acknowledgements. We acknowledge useful discussions with Jens Bardarson, Matt Foster, Cosma Fulga, Igor Gornyi, Alexander Mirlin, Pavel Ostrovsky, and Elio König. Computations were performed at the Ohio Supercomputer Center and the Lawrencium cluster at Lawrence Berkeley National Lab. B.S. acknowledges financial support by the German National Academy of Sciences Leopoldina through grant LPDS 2018-12. E.J.D was supported by NSF Graduate Research Fellowship Program, NSF DGE 1752814. J.E.M. acknowledges support by TIMES at Lawrence Berkeley National Laboratory supported by the U.S. Department of Energy, Office of Basic Energy Sciences, Division of Materials Sciences and Engineering, under Contract No. DE-AC02-76SF00515 and a Simons Investigatorship.

[1] B. Huckestein. *Scaling theory of the integer quantum Hall effect.* Rev. Mod. Phys., **67**, 357 (1995).

[2] F. Evers and A. D. Mirlin. *Anderson transitions.* Rev. Mod. Phys., **80**, 1355 (2008).

[3] J. T. Chalker and P. D. Coddington. *Percolation, quantum tunnelling and the integer Hall effect.* J. Phys. C, **21**, 2665–2679 (1988).

[4] B. Kramer, T. Ohtsuki, and S. Kettemann. *Random network models and quantum phase transitions in two dimensions.* Phys. Rep., **417**, 211–342 (2005).

[5] H. Obuse, A. R. Subramaniam, A. Furusaki, I. A. Gruzberg, and A. W. W. Ludwig. *Boundary Multifractality at the Integer Quantum Hall Plateau Transition: Implications for the Critical Theory.* Phys. Rev. Lett., **101**, 116802 (2008).

[6] F. Evers, A. Mildenberger, and A. D. Mirlin. *Multifractality at the Quantum Hall Transition: Beyond the Parabolic Paradigm.* Phys. Rev. Lett., **101**, 116803 (2008).

[7] K. Slevin and T. Ohtsuki. *Critical exponent for the quantum Hall transition.* Phys. Rev. B, **80**, 041304 (2009).

[8] H. Obuse, A. R. Subramaniam, A. Furusaki, I. A. Gruzberg, and A. W. W. Ludwig. *Conformal invariance, multifractality, and finite-size scaling at Anderson localization transitions in two dimensions.* Phys. Rev. B, **82**, 035309 (2010).

[9] M. Amado, A. V. Malyshev, A. Sedrakyan, and F. Domínguez-Adame. *Numerical study of the localization length critical index in a network model of plateau-plateau transitions in the quantum Hall effect.* Phys. Rev. Lett., **107**, 066402 (2011).

[10] I. Fulga, F. Hassler, A. Akhmerov, and C. Beenakker. *Topological quantum number and critical exponent from conductance fluctuations at the quantum Hall plateau transition.* Phys. Rev. B, **84**, 245447 (2011).

[11] H. Obuse, I. A. Gruzberg, and F. Evers. *Finite-size effects and irrelevant corrections to scaling near the integer quantum Hall transition.* Phys. Rev. Lett., **109**, 206804 (2012).

[12] K. Slevin and T. Ohtsuki. *Finite Size Scaling of the Chalker-Coddington Model.* Int. J. Mod. Phys. Conf. Ser., **11**, 60–69 (2012).

[13] W. Nuding, A. Klümper, and A. Sedrakyan. *Localization length index and subleading corrections in a Chalker-Coddington model: A numerical study.* Phys. Rev. B, **91**, 115107 (2015).

[14] M. Ippoliti, S. D. Geraedts, and R. N. Bhatt. *Integer quantum Hall transition in a fraction of a Landau level.* Phys. Rev. B, **97**, 014205 (2018).

[15] Q. Zhu, P. Wu, R. N. Bhatt, and X. Wan. *Localization-length exponent in two models of quantum Hall plateau transitions.* Phys. Rev. B, **99**, 024205 (2019).

[16] M. Puschmann, P. Cain, M. Schreiber, and T. Vojta. *Integer quantum Hall transition on a tight-binding lattice.* Phys. Rev. B, **99**, 121301 (2019).

[17] M. Puschmann, P. Cain, M. Schreiber, and T. Vojta. *Edge state critical behavior of the integer quantum Hall transition.* arXiv e-prints, arXiv:2004.01611 (2020).

[18] J. P. Dahlhaus, J. M. Edge, J. Tworzydło, and C. W. J. Beenakker. *Quantum Hall effect in a one-dimensional dynamical system.* Phys. Rev. B, **84**, 115133 (2011).

[19] Z. Wang, B. Jovanović, and D.-H. Lee. *Critical Conductance and Its Fluctuations at Integer Hall Plateau Transitions.* Phys. Rev. Lett., **77**, 4426 (1996).

[20] L. Schweitzer and P. Markoš. *Universal conductance and conductivity at critical points in integer quantum hall systems.* Phys. Rev. Lett., **95**, 256805 (2005).

[21] R. Bondesan, D. Wieczorek, and M. R. Zirnbauer. *Pure scaling operators at the integer quantum Hall plateau transition.* Phys. Rev. Lett., **112**, 186803 (2014).

[22] R. Bondesan, D. Wieczorek, and M. R. Zirnbauer. *Gaussian free fields at the integer quantum Hall plateau transition.* Nuclear Physics B, **918**, 52–90 (2017).

[23] M. R. Zirnbauer. *The integer quantum Hall plateau transition is a current algebra after all.* Nucl. Phys. B, **941**, 458 (2019).

[24] B. Sbierski, J. F. Karcher, and M. S. Foster. *Spectrum-Wide Quantum Criticality at the Surface of Class AIII Topological Phases: An "Energy Stack" of Integer Quantum Hall Plateau Transitions.* Phys. Rev. X, **10**, 021025 (2020).

[25] A. W. W. Ludwig, M. P. A. Fisher, R. Shankar, and G. Grinstein. *Integer quantum Hall transition: An alternative approach and exact results.* Phys. Rev. B, **50**, 7526 (1994).

[26] F. Haldane. *Model for a quantum Hall effect without Landau levels: Condensed-matter realization of the "parity anomaly".* Phys. Rev. Lett., **61**, 2015 (1988).

[27] M. R. Zirnbauer. *Riemannian symmetric superspaces and their origin in random-matrix theory.* J. Math. Phys., **37**,

4986 (1996).

[28] A. Altland and M. R. Zirnbauer. *Nonstandard symmetry classes in mesoscopic normal-superconducting hybrid structures.* Phys. Rev. B, **55**, 1142 (1997).

[29] C. Ho and J. Chalker. *Models for the integer quantum Hall effect: The network model, the Dirac equation, and a tight-binding Hamiltonian.* Phys. Rev. B., **54**, 8708 (1996).

[30] See Supplemental Material [url] for non-rigorous arguments for the equivalence of IQHT and DDF criticality, details on the fitting procedure for quasi-1d Lyapunov exponents, on the alternative scaling observable, Landauer conductance and Drude conductivity. The supplemental material contains references Klumper2019,Janssen-1999,Klesse-2001,Gruzberg-Classification-2013,Jovanovi c1998.

[31] C.-Z. Chang, J. Zhang, X. Feng, J. Shen, Z. Zhang, M. Guo, K. Li, Y. Ou, P. Wei, L.-L. Wang, Z.-Q. Ji, Y. Feng, S. Ji, X. Chen, J. Jia, X. Dai, Z. Fang, S.-C. Zhang, K. He, Y. Wang, L. Lu, X.-C. Ma, and Q.-K. Xue. *Experimental Observation of the Quantum Anomalous Hall Effect in a Magnetic Topological Insulator.* Science, **340**, 167–170 (2013).

[32] C.-X. Liu, S.-C. Zhang, and X.-L. Qi. *The Quantum Anomalous Hall Effect: Theory and Experiment.* Annual Review of Condensed Matter Physics, **7**, 301–321 (2016).

[33] M. Serlin, C. L. Tschirhart, H. Polshyn, Y. Zhang, J. Zhu, K. Watanabe, T. Taniguchi, L. Balents, and A. F. Young. *Intrinsic quantized anomalous Hall effect in a moiré heterostructure.* Science, **367**, 900–903 (2020).

[34] C.-Z. Chang, W. Zhao, J. Li, J. K. Jain, C. Liu, J. S. Moodera, and M. H. W. Chan. *Observation of the Quantum Anomalous Hall Insulator to Anderson Insulator Quantum Phase Transition and its Scaling Behavior.* Phys. Rev. Lett., **117**, 126802 (2016).

[35] M. Kawamura, M. Mogi, R. Yoshimi, A. Tsukazaki, Y. Kozuka, K. S. Takahashi, M. Kawasaki, and Y. Tokura. *Current scaling of the topological quantum phase transition between a quantum anomalous Hall insulator and a trivial insulator.* Phys. Rev. B, **102**, 041301 (2020).

[36] A. Schuessler, P. Ostrovsky, I. Gornyi, and A. Mirlin. *Analytic theory of ballistic transport in disordered graphene.* Phys. Rev. B, **79**, 075405 (2009).

[37] B. Sbierski and C. Fräßdorf. *Strong disorder in nodal semimetals: Schwinger-Dyson-Ward approach.* Phys. Rev. B, **99**, 020201 (2019).

[38] B. Kramer and A. McKinnon. *Localization: theory and experiment.* Rep. Prog. Phys., **56**, 1469 (1993).

[39] M. Amado, A. V. Malyshev, A. Sedrakyan, and F. Domínguez-Adame. *Numerical study of the localization length critical index in a network model of plateau-plateau transitions in the quantum hall effect.* Phys. Rev. Lett., **107**, 066402 (2011).

[40] J. Bardarson, J. Tworzydlo, P. Brouwer, and C. Beenakker. *One-Parameter Scaling at the Dirac Point in Graphene.* Phys. Rev. Lett., **99**, 106801 (2007).

[41] X.-l. Qi, Y.-s. Wu, and S.-c. Zhang. *Topological quantization of the spin Hall effect in two-dimensional paramagnetic semiconductors.* Phys. Rev. B, **74**, 085308 (2006).

[42] C. Groth, M. Wimmer, A. Akhmerov, and X. Waintal. *Kwant: a software package for quantum transport.* New J. Phys., **16**, 063065 (2014).

[43] J. Tworzydlo, B. Trauzettel, M. Titov, A. Rycerz, and C. W. J. Beenakker. *Quantum-limited shot noise in graphene.* Phys. Rev. Lett., **96**, 246802 (2006).

[44] P. M. Ostrovsky, I. V. Gornyi, and A. D. Mirlin. *Quantum criticality and minimal conductivity in graphene with long-range disorder.* Phys. Rev. Lett., **98**, 256801 (2007).

[45] A. M. M. Pruisken. *On localization in the theory of the quantized hall effect: A two-dimensional realization of the θ-vacuum.* Nucl. Phys. B., **235**, 277 (1984).

[46] H. Weidenmüller. *Single electron in a random potential and a strong magnetic field.* Nucl. Phys. B., **290**, 87 (1987).

[47] N. Read (1991). Unpublished.

[48] M. R. Zirnbauer. *Towards a theory of the integer quantum Hall transition: From the nonlinear sigma model to superspin chains.* Annalen Phys., **3**, 513–577 (1994). [Erratum: Annalen Phys. **4**, 89 (1995)].

[49] K. Nomura, S. Ryu, M. Koshino, C. Mudry, and A. Furusaki. *Quantum Hall Effect of Massless Dirac Fermions in a Vanishing Magnetic Field.* Phys. Rev. Lett., **100**, 246806 (2008).

[50] J. Cardy. *Scaling and Renormalization in Statistical Physics* (1996).

[51] M. R. Zirnbauer. *Logarithmic scaling at the integer quantum Hall plateau transition.* Talk presented at the "Localisation 2020" conference (2020).

[52] E. J. Dresselhaus, B. Sbierski, and I. Gruzberg. *Numerical evidence for marginal scaling at the integer quantum Hall transition.* Arxiv, **2101.01716** (2021).

[53] A. Klümper, W. Nuding, and A. Sedrakyan. *Random network models with variable disorder of geometry.* Phys. Rev. B, **100**, 140201 (2019).

[54] M. Janssen, M. Metzler, and M. Zirnbauer. *Point-contact conductances at the quantum Hall transition.* Phys. Rev. B., **24**, 15836 (1999).

[55] R. Klesse and M. Zirnbauer. *Point-Contact Conductances from Density Correlations.* Phys. Rev. Lett., **86**, 2094 (2000).

[56] I. A. Gruzberg, A. D. Mirlin, and M. R. Zirnbauer. *Classification and symmetry properties of scaling dimensions at Anderson transitions.* Phys. Rev. B, **87**, 125144 (2013).

[57] B. Jovanovic and Z. Wang. *Conductance Correlations near Integer Quantum Hall Transition.* Phys. Rev. Lett., **81**, 2767 (1998).